Effect of perturbations on the kagome S=12 antiferromagnet at all temperatures

Bernard Bernu, Laurent Pierre, Karim Essafi, Laura Messio

Effect of perturbations on the kagome $S = 1/2$ antiferromagnet at all temperatures

Bernard Bernu,[1] Laurent Pierre,[2] Karim Essafi,[1] and Laura Messio[1, 3]

[1]*Sorbonne Université, CNRS, Laboratoire de Physique Théorique de la Matière Condensée, LPTMC, F-75005 Paris, France*[∗]

[2]*Paris X, Nanterre*

[3]*Institut Universitaire de France (IUF), F-75005 Paris, France*[†]

(Dated: January 8, 2020)

The ground state of the $S = 1/2$ kagome Heisenberg antiferromagnet is now recognized as a spin liquid, but its precise nature remains unsettled, even if more and more clues point towards a gapless spin liquid. We use high temperature series expansions (HTSE) to extrapolate the specific heat $c_V(T)$ and the magnetic susceptibility $\chi(T)$ over the full temperature range, using an improved entropy method with a self-determination of the ground state energy per site e_0. Optimized algorithms give the HTSE coefficients up to unprecedented orders (20 in $1/T$) and as exact functions of the magnetic field. Three extrapolations are presented for different low-T behaviors of c_V: exponential (for a gapped system), linear or quadratic (for two different types of gapless spin liquids). We study the effects of various perturbations to the Heisenberg Hamiltonian: Ising anisotropy, Dzyaloshinskii-Moriya interactions, second and third neighbor interactions, and randomly distributed magnetic vacancies. We propose an experimental determination of $\chi(T = 0)$, which could be non zero, from c_V measurements under different magnetic fields.

I. INTRODUCTION

The physics of the spin $S = 1/2$ kagome lattice, with first neighbor Heisenberg antiferromagnetic interactions[1] (KHAF) has recently known two major progresses. One is experimental, with the realization of high quality crystals of Herbersmithite[2], opening the possibility of precise measurements[3,4]; the other is numerical, with the understanding of the bias tending to erroneously favor a gapped spin liquid (SL) ground state in DMRG simulations[5–7]. A gapless SL ground state is now almost a consensus, supported by recent precise measurements of the low-T magnetic susceptibility[4]. However, there remain several types of bidimensional gapless SL, among which the $U(1)$ SL (with a ponctual Fermi surface) and the Fermi SL (with a linear Fermi surface)[8]. They distinguish themselves notably by the low-T behavior of their specific heat: a linear behavior, $c_V \propto T$, is a characteristic of a Fermi SL, whereas a quadratic one, $c_V \propto T^2$, is an indication of a $U(1)$ SL (to compare to $c_V \propto T^2 e^{-\Delta/T}$ for a gapped phase, where Δ is the gap). We label these different cases by an integer $\alpha = 1$ or 2 in the gapless cases ($c_V \propto T^\alpha$) and $\alpha = 0$ in the gapped case. Up to now, neither the experimental nor the theoretical works are able to determine α for the KHAF, even if recent theoretical and experimental results seem to indicate that $\alpha \neq 0$.

But all these considerations pre-suppose that Herbertsmithite is effectively described by a KHAF on perfect and independent kagome planes. In reality, this model suffers from several perturbations: dilution, Ising anisotropy, Dzyaloshinskii-Moriya (DM) interactions, further neighbor interactions... Previous studies show that their effects on the ideal Hamiltonian are moderate: whatever the phase of the KHAF ground state, it seems stable for small values of these perturbations. However, they can quantitatively influence the finite temperature thermodynamic measurements. Thus, we use in this article high temperature series expansions (HTSE) to explore the finite temperature effects of a magnetic field h and of all the previously listed perturbations in the three cases $\alpha = 0$, 1 or 2. It illustrates the difficulty to fit experimental data for many free parameters and without knowing α. However, we extract from all these results a way to determine the zero temperature magnetic susceptibility χ_0 from c_V measurements under different h, and we anticipate the synthesis of parent compounds of Herbertsmithite with tunable perturbations to KHAF.

HTSE exactly calculates the Taylor coefficients of thermodynamic quantities in powers of the inverse temperature $\beta = 1/T$. From these coefficients, one can reliably and easily reconstruct the quantities from infinite down to moderate temperatures of the order of the interaction strength, using either the raw series, Padé approximants (PAs), or methods as differential Padé approximants, Euler transformation, ...[9–12]. When there is no singularity down to $T = 0$ in the thermodynamic functions (i.e. no phase transition, as notably in SL phases), it is possible to extrapolate HTSE over the full range of temperature. In this case, the entropy method combines HTSE with an hypothesis on α to get thermodynamic quantities as the specific heat per site c_V or the magnetic susceptibility per site χ[13–15]. This method, thereafter denoted HTSE+$s(e)$, is fully relevant to extract the Hamiltonian parameters from experimental results[16–19].

We get in this article HTSE coefficients up to an order notably larger than previously[14], in the presence of all the above interactions and with an exact dependency in h. Moreover, we present here the extrapolations on the KHAF supposing a *gapless* spin liquid, with a special emphasis on χ and c_V (see also ref.[20] on c_V), which can be measured experimentally[4]. These extrapolations require input parameters: α, the ground state energy per site e_0

and χ_0. Often, α is known, as for Néel or gapped ground state. Except for ferromagnetic states, $e_0(h)$ and $\chi_0 = -d^2 e_0/dh^2$ are usually unknown. We present here a new method of self-determination of e_0 that overcome this obstacle. In Sec. II, we present the results of raw series. We then discuss the extrapolation method and present the results on the perfect KHAF in Sec. III. Sec. IV is devoted to the study of several perturbations, followed by the effects of a magnetic field h. Concluding remarks are in the last section. Supplemental material[21] gives details on HTSE+$s(e)$ and furnish more figures illustrating the effect of the perturbations.

II. RAW HTSE COEFFICIENTS WITH EXACT DEPENDENCY IN h

We first focus on the raw series of the thermodynamic limit of the logarithm of the partition function $\lim_{N\to\infty} \frac{\ln Z}{N}$ in powers of β with, as first main result of this article, their obtention as exact functions of h.

The KHAF Hamiltonian $\mathcal{H}$ consists in spins $S = 1/2$ on a kagome lattice, in presence of an arbitrary magnetic field h (times a factor $g\mu_B$, set to 1 in the following), with antiferromagnetic interactions on all pairs of nearest neighbors:

$$\mathcal{H}_0 = J_1 \sum_{\langle i,j \rangle} \boldsymbol{S}_i \cdot \boldsymbol{S}_j, \qquad \mathcal{H} = \mathcal{H}_0 - hS^z, \qquad (1)$$

where $S^z = \sum_i S_i^z$ is the total spin along the z direction and $\mathbf{S}_i$ the spin operator on site i. J_1 is set to unity in the following. The partition function is:

$$Z = \operatorname{Tr} e^{-\beta\mathcal{H}} = \sum_{n=0}^{\infty} \frac{(-\beta)^n}{n!} \operatorname{Tr}(\mathcal{H}^n). \qquad (2)$$

After keeping the part of the traces $\operatorname{Tr}(\mathcal{H}^n)$ originating from connected clusters with n links on the lattice, it gives us the following HTSE in powers of β, where coefficients are finite order polynomials of h^2:

$$\lim_{N\to\infty} \frac{\ln Z}{N} = \ln 2 + \sum_{n=1}^{\infty} \left(\sum_{k=0}^{n/2} Q_{n,k} h^{2k} \right) \beta^n. \qquad (3)$$

The first coefficients $Q_{n,0}$ and $Q_{n,1}$ are related to the HTSE of respectively c_V and χ at $h = 0$, and are the only ones that were calculated up to now[13,14,20]: the effects of a finite h were unaccessible (some further terms were calculated for other models[13,22], without being exploited or still strongly limiting the possible values of h).

Beside the now exact treatment of h, we get access to unprecedented orders despite the exponential complexity of the calculations. $Q_{n,k}$ are determined for n up to 20, against 17 previously[14]. Fig. 1 shows that the raw HTSE diverges below T=1, while the PAs converge down to 0.5 allowing to describe the main peak of c_V.
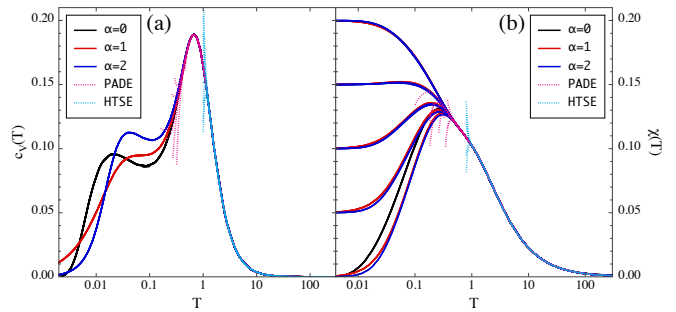

FIG. 1. Results from HTSE+$s(e)$ at order 20 in β for $h = 0$ on the KHAF. (a) Specific heat c_V; Gapped ($\alpha = 0$, black lines) and gapless ground states ($\alpha = 1$, red lines, and 2, blue lines) are considered and e_0 is fixed to -0.4372, -0.4384 and -0.4395 respectively. Dashed cyan lines are the raw HTSE of orders 13 through 20. Dashed magenta lines are the PAs $d = 6$ through 14 of HTSE at order 20. (b) Same as in (a) for the magnetic susceptibility χ. Several scenario for the χ_0 value are presented.

III. EXTRAPOLATION OVER THE FULL TEMPERATURE RANGE

In the thermodynamic limit, canonical and microcanonical ensembles are equivalent. It implies that the information contained in $Z(T,h)$ is the same as in the entropy per spin $s(e,h)$, with e the energy per spin. At fixed h, s and e are monotonous functions of T, going from $e_0(h)$ and $s_0 = 0$ at $T = 0$, to $e_\infty = 0$ and $s_\infty = \ln(2S+1)$ at $T = \infty$. These constraints near $e_0(h)$ are equivalent to the two sum rules on c_V, but more easily imposed on $s(e,h)$[13]. Moreover, the behavior of $s(e,h)$ for $e \to e_0(h)$ can be infered from the (known or supposed) low energy properties of the model. Thus, we work in the microcanonical ensemble[13,14,20]. From the HTSE, Eq. (3), we deduce the series expansion of $s(e,h)$ around e_∞ and extrapolate this function over the full interval $[e_0(h), e_\infty]$. To remove the singularity of s at e_0, we introduce an auxiliary function $G_\alpha(s(e,h))$. Then, PAs of this function of e are used to reconstruct s[21].

This HTSE+$s(e)$ procedure requires the knowledge of $e_0(h)$. We define $e_{00} = e_0(h = 0)$. As no numerical method is currently able to give it to the required precision, we browse a range of values and select the one that gives the most coinciding results for $h = 0$[21]. This leads to values near the ones infered from DMRG ($e_{00} = -0.4386(5)$)[23–25] and exact diagonalization ($e_{00} = -0.4387039$ for a 48 site cluster)[25,26].

For small $h \neq 0$, the energy is given by

$$e_0(h) \simeq e_{00} - \frac{1}{2}\chi_0 h^2, \qquad (4)$$

as thermodynamic relations imply that $\chi_0 = \chi(T = 0, h = 0) = -\frac{d^2 e_0(h)}{dh^2}$. While χ_0 is 0 in gapped systems, as the ground state remains unchanged for infinitesimal h, we a priori have $\chi_0 \neq 0$ for gapless systems. To give an idea of the χ_0 value, we can look at the classical model[27],
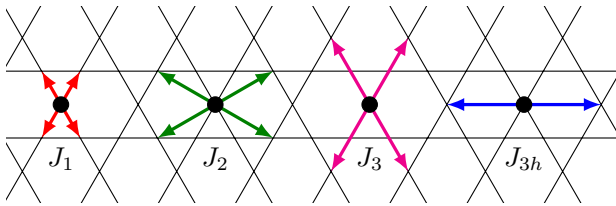
FIG. 2. First (J_1), second (J_2) and third (J_3 and J_{3h}) neighbor interactions on the kagome lattice.

which is gapless: $\chi_0 = S/6$. A recent ED study[28] uses the energy in different spin sectors and for different lattice sizes to get a possibly finite χ_0, which is also compatible with sine-square deformation results[29]. We choose here to consider χ_0 as an input parameter and to deduce $e_0(h)$ from e_{00} and χ_0. Another possibility is to self-determine $e_0(h)$ and to extract χ_0 from it, but this is not conclusive. Indeed, our procedure (see Sec. II.E of[21]) allows a determination of $e_0(h)$ with some uncertainties and χ_0, being related to the second derivative of $e_0(h)$, suffers for even much larger uncertainties; therefore, we find that almost any reasonable value of χ_0 is compatible with our results.

We note s' and s'' the derivatives of s with respect to e at constant h. We recall that $\beta = s'$. The specific heat per site c_V and magnetization per site m are:

$$c_V = -\frac{s'^2}{s''}, \qquad m = \frac{1}{s'}\left.\frac{\partial s}{\partial h}\right|_e. \qquad (5)$$

We emphasize that m is now obtained directly from $s(e,h)$, simplifying the procedure used in[14]. We deduce from m the experimentally measured magnetic susceptibility per site $\chi = m/h$.

At the end of the day, for a given spin model, we extrapolate $\chi(T)$ and $c_V(T)$ at all temperatures from the HTSE, with, as supplementary input, the values of e_0, χ_0, and α. Fig. 1 shows c_V and χ for the unperturbed Hamiltonian of Eq. (1). The assumption on α has no influence for $T > 0.3$: HTSE strongly constrain the functions in this domain of temperature. Notably, the high temperature peak of c_V near $T = 0.7$ is well determined, which is not the case for the small temperature secondary peak ($T \simeq 0.03$). The existence of such a peak or shoulder, sign of a large amount of low energy states, is still highly debated as it is very sensible to eventual finite size effects[30,31].

At this point, it is important to emphasize a particularity of the KHAF. In most of simpler models, we are not able to get convincing results if we arbitrarily chose α or e_0, in the sense where we do not get several mingled PAs for $G_\alpha(e,h)$: only physically correct hypothesis give a collection of coinciding PAs. In this respect, KHAF is very special as any hypothesis on α leads to valuable extrapolations: no α can be discarded by this way.
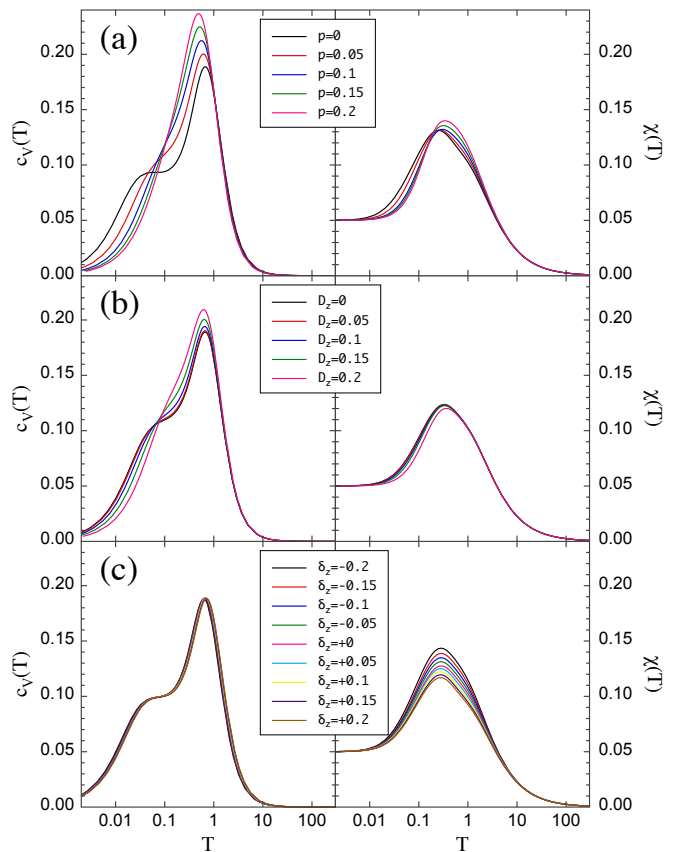

FIG. 3. HTSE+$s(e)$ results on the KHAF: specific heat c_V and magnetic susceptibility χ for different (a) vacancy rates p, (b) DM interactions D_z and (c) Ising anisotropy δ_z. Results for $\alpha = 1$ (linear low T c_V) and for $\chi_0 = 0.05$ are shown. The results for $\alpha = 0$ or 2 and for other χ_0 are in[21].

IV. RESULTS FOR THE MODIFIED KHAF

We now add different terms to $\mathcal{H}_0$, whose effects will be studied successively below:

$$\mathcal{H} = \mathcal{H}_0 - h\sum_i S_i^z + \sum_{\langle i,j\rangle}\left(D_z \cdot (\mathbf{S}_i \wedge \mathbf{S}_j)_z + \delta_z S_i^z S_j^z\right) \quad (6)$$

$$+ J_2 \sum_{\langle i,j\rangle_2} \mathbf{S}_i \cdot \mathbf{S}_j + J_3 \sum_{\langle i,j\rangle_3} \mathbf{S}_i \cdot \mathbf{S}_j + J_{3h} \sum_{\langle i,j\rangle_{3h}} \mathbf{S}_i \cdot \mathbf{S}_j,$$

where D_z is the z component of the DM vector, δ_z the Ising anisotropy, J_2, J_3 and J_{3h} the second and third nearest-neighbor terms (see Fig. 2). The $Q_{n,k}$ of Eq. (3) are now polynomials of order n in the rate of vacancies p, D_z, δ_z, J_2 and J_{3h}. The HTSE order depends on the complexity of the Hamiltonian: order 20 is obtained for the KHAF with impurities, 18 with the Ising anisotropy, 16 with DM interactions, 15 with second and third neighbor exchanges.

Fig. 3 shows the influence on c_V and χ of some of these perturbations and of a dilution rate, for $h = 0$ and with the hypothesis that $\alpha = 1$. To get χ, we need a supplementary hypothesis on χ_0, chosen to be 0.05 for this fig-
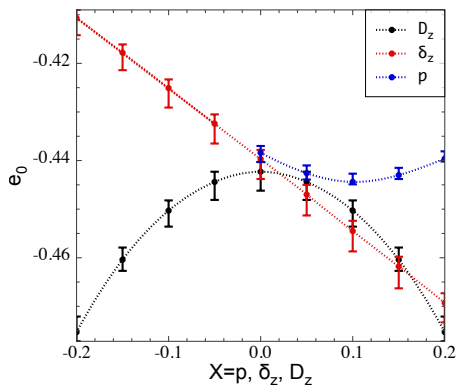
FIG. 4. Ground state energies e_0 for different impurity rates p, DM interaction strength D_z and Ising anisotropy δ_z, for $\alpha = 1$. The results differ at $X = 0$ (pure KHAF) due to the different HTSE orders used for the various types of perturbations X.

ure (results for other values are in[21]). Note that at intermediate temperatures, our results are consistent with Numerical Linked Cluster (NLC) results[32,33]. Fig.4 shows how the ground state energy, e_0, extracted from the most coinciding HTSE+$s(e)$ extrapolations[21], evolves with the considered perturbations.

Impurities. The rate of vacancies (magnetic Cu replaced by non magnetic Zn atoms) in the kagome lattice of Herbertsmithite is experimentally estimated to be less than 5%[4]. We suppose here that interactions between remaining spins are unchanged. The extracted $e_0(p)$ has a minimum around $p = 10\%$ (Fig. 4). For classical spins, a low p does not modify the energy per *magnetic site*[34] (even if it lowers the energy per *lattice site*) and this minima cannot be reproduced. But for quantum $1/2-$spins[35–37], it can be qualitatively understood as the minimal energies E_t on a triangle and E_b on a bond are the same ($-3/4$), whereas classically, $E_t < E_b$ ($-3S^2/2$ against $-S^2$). A rough approximation of the energy per spin on the lattice is

$$\frac{2(1-p)^2}{3}E_t + 2(1-p)pE_b$$

and reproduces the minimum at $p \simeq 10\%$ if $E_t \simeq 4E_b/3$, which seems reasonable.

At finite temperature, we find that impurities soften the separation of the two peaks in c_V, strengthen χ and shift it to higher temperatures (Fig. 3(a)). Another type of defects is present in Herbertsmithite but not treated here: interlayer magnetic atoms (Zn replaced by Cu atoms) at a rate of 15% of occupation[4,38]. They will enforce the tridimensional character of the compound.

Dzyaloshinskii-Moriya interaction. This interaction originates from the spin-orbit coupling[39,40] and is often considered, in Herbertsmithite, as the main deviation from the KHAF, together with impurities[36]. The out of plane component D_z is supposed to be dominant and is the only one considered here. The combined effect of the in and out of plane **D** has been studied by

NLC[32,33]. The sum in the Hamiltonian (6) is over oriented links, all pointing in the same arbitrary direction when we turn around the lattice hexagons. In Herbertsmithite, $D_z \simeq 0.04 J_1$[41]. Order is supposed to appear for $D_z \simeq 0.08 J_1$[42–44], even if smaller values ($D_z \simeq 0.01 J_1$) have recently been proposed[45]. We find that D_z enhances the main c_V peak and has a weak effect on χ (Fig. 3(b)). As expected, $e_0(D_z)$ behaves quadratically (Fig 4).

Ising anisotropy. The Ising anisotropy δ_z interpolates between the ferromagnetic Ising model ($\delta_z = -\infty$), the XY model ($\delta_z = -1$) and the antiferromagnetic Ising model ($\delta_z = \infty$), staying in the same spin liquid phase for $\delta_z > -1$[46]. Moreover, an exactly solvable point $\delta_z = -3/2$ was recently discovered and analyzed[47]. For small δ_z, $e_0(\delta_z)$ is linear (Fig 4). This can be qualitatively understood by considering that most of the energy contribution in the ground state comes from the concentration c of singlet bonds, whose energy is $-(3+\delta_z)/4$. With this naive picture, we get $e_0(\delta_z) = e_0(\delta_z = 0)(1+\delta_z/3)$, whose slope is in agreement with the one fitted from HTSE data $0.146(1) \sim -0.44/3$ (Fig. 4). Similarly, the susceptibility of such singlets decreases when δ_z increases and reciprocally, which is the behavior seen in Fig. 3(c). On the contrary, c_V is almost insensitive to δ_z.

Second and third neighbors interactions. J_2, J_3 and J_{3h} are known to lift the classical degeneracy of the KHAF toward the $\sqrt{3} \times \sqrt{3}$ long range order for $J_2 < 0$ and $J_3 > 0$, towards the $q = 0$ order for $J_2 > 0$, $J_3 < 0$ and $J_{3h} < 0$ and towards the cuboc1 order for $J_{3h} > 0$[44,48]. For quantum spins $1/2$, small changes in these parameters have seemingly low influence and preserve the spin liquid phase for $|J_2|, |J_{3h}| \leq 0.2$[49–52]. The J_3 case is less studied. These terms add new links to the KHAF model, therefore HTSE are limited to order 15. J_2 and J_3 have stronger effects than J_{3h} on $c_V(T)$ and $\chi(T)$. Results are displayed and discussed in[21] for completeness.

Magnetic field. We now consider the effect of a magnetic field h, that is a special perturbation as it is easily tunable experimentally, contrarily to the previous ones. Up to now, HTSE coefficients were only computed at the lowest order in h but are here exact. In a gapless system, the ground state magnetization continuously increases up to a critical field h_c, above which the phase changes, either towards the fully magnetized state, or towards an intermediate phase. For classical spins[27], $h_c = 2S$ at $T = 0$, giving rise to the finite T $\frac{1}{3}$-magnetization plateau, but quantum studies[53] find a lowest $\frac{1}{9}$-magnetization plateau for $h_c \simeq 0.6S$. Thus, we focus on $h \lesssim 0.2$. However, for Herbersmithite where $J \simeq 180K$, $h \sim 0.1$ is a hardly achieved field for experimentalists. On Fig. 5, the difference $(c_V(T,h) - c_V(T,h=0))/h^2$ appears to be weakly dependent on h, but roughly proportional to the difference $\chi_0 - 0.15$. This is an interesting effect, that could be used to get an hint on the χ_0 value as the phonons contributions, known to spoil the c_V measurements, are a priori suppressed in this difference.
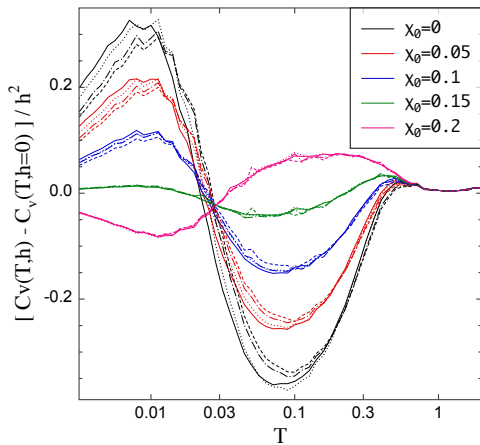
FIG. 5. Variation of the specific heat $c_V(T)$ using various values of χ_0. Shown are $(c_V(T, h) - c_V(T, h = 0))/h^2$ for $\alpha = 1$ and several values of h: 0.2 (full lines), 0.15 (dotted lines) 0.1 (dahed-dotted lines) and 0.05 (dashed lines). By construction, the integral of each curve is 0. For $\chi_0 = 0.15$, the curve is almost flat. For $\chi_0 < 0.15$, there is an increase of $c_V(T)$ at $T \lesssim 0.03$ and a decrease for $0.03 \gtrsim T \gtrsim 0.3$, and the opposite for $\chi_0 > 0.15$.

V. CONCLUSION

In this paper, the HTSE coefficients of antiferromagnetic 1/2-spins on the kagome lattice have been exactly obtained as polynomials of various Hamiltonian parameters, with at least three more terms than previously. The entropy method (HTSE+$s(e)$) has been applied to these models. Two types of gapless spin liquids (linear and quadratic low T specific heat) have been considered and several values of χ_0 have been explored. We have studied the effect on c_V and χ of various perturbations of the KHAF: magnetic field, impurities, DM interaction, Ising anisotropy, further neighbor couplings. The ground state

energies have been extracted with a procedure based on the number of coinciding PAs detailed the supplemental material[21], leading to coherent results down to small temperatures.

The variations of $c_V(T)$ and $\chi(T)$ are sensible to Hamiltonian perturbations below $T \sim J_1/10$. For Herbertsmithite, this is precisely in this range of temperature that the experimentalists get more and more precise data, therefore HTSE+$s(e)$ is a powerful tool to determine the values of the Hamiltonian parameters from them, as already demonstrated for other models. We notably enlightened a way to probe χ_0 using c_V measurements at finite T under a magnetic field. In a near future, we expect that measurements under pressure of kagome compounds will tune some other Hamiltonian parameters, and that the impurity rate will be controlled.

We have here treated in great details the controversial case of the KHAF, but our extrapolation technic can as well treat any statistical model if the HTSE coefficients are known. Our code calculating the HTSE coefficients works for spin models on any lattice, for any interaction preserving the total magnetization along z and for $S = 1/2$. What has been chosen as perturbative parameters in this paper can be set to any arbitrary value as the HTSE coefficients are exact polynomials of them. However, the convergence properties of the series are affected by possible phase transitions.

[*] bernu@lptmc.jussieu.fr

[†] messio@lptmc.jussieu.fr

[1] Philippe Mendels and Fabrice Bert, "Quantum kagome frustrated antiferromagnets: One route to quantum spin liquids," Comptes Rendus Physique **17**, 455 – 470 (2016).

[2] T. H. Han, J. S. Helton, S. Chu, A. Prodi, D. K. Singh, C. Mazzoli, P. Müller, D. G. Nocera, and Y. S. Lee, "Synthesis and characterization of single crystals of the spin-$\frac{1}{2}$ kagome-lattice antiferromagnets $Zn_xCu_{4-x}(OH)_6Cl_2$," Phys. Rev. B **83**, 100402(R) (2011).

[3] T.-H. Han, J. S. Helton, S. Chu, D. G. Nocera, J. A. Rodriguez-Rivera, C. Broholm, and Y. S. Lee, "Fractionalized excitations in the spin-liquid state of a kagome-lattice antiferromagnet," Nature **492**, 406–410 (2012).

[4] P. Khuntia, Q. Barthélemy, F. Bert, E. Kermarrec, B. Bernu, L. Messio, A. Zorko, M. Velazquez, and P. Mendels, "Gapless ground state in the archetypal quantum kagome antiferromagnet $ZnCu_3(OH)_6Cl_2$,".

[5] Yin-Chen He, Michael P. Zaletel, Masaki Oshikawa, and Frank Pollmann, "Signatures of Dirac Cones in a DMRG Study of the Kagome Heisenberg Model," Phys. Rev. X **7**, 031020 (2017).

[6] H. J. Liao, Z. Y. Xie, J. Chen, Z. Y. Liu, H. D. Xie, R. Z. Huang, Bruce Normand, and T. Xiang, "Gapless Spin-Liquid Ground State in the S-1/2 Kagome Antiferromagnet," Phys. Rev. Lett. **118**, 137202 (2017).

[7] Arnaud Ralko, Frédéric Mila, and Ioannis Rousochatzakis, "Microscopic theory of the nearest-neighbor valence bond sector of the spin-$\frac{1}{2}$ kagome antiferromagnet," Phys. Rev. B **97**, 104401 (2018).

[8] Ying Ran, Michael Hermele, Patrick A. Lee, and Xiao-Gang Wen, "Projected-Wave-Function Study of the Spin-1/2 Heisenberg Model on the Kagomé Lattice," Phys. Rev. Lett. **98**, 117205 (2007).

[9] Jaan Oitmaa and E. Bornilla, "High-temperature-series study of the spin-1/2 Heisenberg ferromagnet," Phys. Rev.

B **53**, 14228–14235 (1996).

[10] M. Roger, "Differential approximants: An accurate interpolation from high-temperature series expansions to low-temperature behavior in two-dimensional ferromagnets," Phys. Rev. B **58**, 11115–11118 (1998).

[11] Andre Lohmann, Heinz-Jürgen Schmidt, and Johannes Richter, "Tenth-order high-temperature expansion for the susceptibility and the specific heat of spin-s Heisenberg models with arbitrary exchange patterns: Application to pyrochlore and kagome magnets," Phys. Rev. B **89**, 014415 (2014).

[12] Andreas Hehn, Natalija van Well, and Matthias Troyer, "High-temperature series expansion for spin-1/2 Heisenberg models," Comput. Phys. Commun. **212**, 180–188 (2017).

[13] Bernard Bernu and G. Misguich, "Specific heat and high-temperature series of lattice models: Interpolation scheme and examples on quantum spin systems in one and two dimensions," Phys. Rev. B **63**, 134409 (2001).

[14] Bernard Bernu and C. Lhuillier, "Spin Susceptibility of Quantum Magnets from High to Low Temperatures," Phys. Rev. Lett. **114**, 057201 (2015).

[15] Heinz-Jürgen Schmidt, Andreas Hauser, Andre Lohmann, and Johannes Richter, "Interpolation between low and high temperatures of the specific heat for spin systems," Phys. Rev. E **95**, 042110 (2017).

[16] G. Misguich, B. Bernu, and L. Pierre, "Determination of the exchange energies in Li_2VOSiO_4 from a high-temperature series analysis of the square-lattice J_1-J_2 Heisenberg model," Phys. Rev. B **68**, 113409 (2003).

[17] J.-C. Orain, B. Bernu, P. Mendels, L. Clark, F. H. Aidoudi, P. Lightfoot, R. E. Morris, and F. Bert, "Nature of the Spin Liquid Ground State in a Breathing Kagome Compound Studied by NMR and Series Expansion," Phys. Rev. Lett. **118**, 237203 (2017).

[18] B. Bernu, C. Lhuillier, E. Kermarrec, F. Bert, P. Mendels, R. H. Colman, and A. S. Wills, "Exchange energies of kapellasite from high-temperature series analysis of the kagome lattice $J_1 - J_2 - J_d$ Heisenberg model," Phys. Rev. B **87**, 155107 (2013).

[19] B. Fåk, E. Kermarrec, L. Messio, B. Bernu, C. Lhuillier, F. Bert, P. Mendels, B. Koteswararao, F. Bouquet, J. Ollivier, A. D. Hillier, A. Amato, R. H. Colman, and A. S. Wills, "Kapellasite: A Kagome Quantum Spin Liquid with Competing Interactions," Phys. Rev. Lett. **109**, 037208 (2012).

[20] G. Misguich and Bernard Bernu, "Specific heat of the S=1/2 Heisenberg model on the kagome lattice: High-temperature series expansion analysis," Phys. Rev. B **71**, 014417 (2005).

[21] See Supplemental Material for further details on the derivation of the main formulae of this article.

[22] Kunihiko Yamaji and Jun Konda, "On the High-Temperature Susceptibilities of the Two-Dimensional Ferromagnetic Heisenberg Spin Systems," Journal of the Physical Society of Japan **35**, 25–32 (1973).

[23] S.g Yan, D. A. Huse, and S. R. White, "Spin-Liquid Ground State of the S = 1/2 Kagome Heisenberg Antiferromagnet," Science **332**, 1173–1176 (2011).

[24] Stefan Depenbrock, Ian P. McCulloch, and Ulrich Schollwöck, "Nature of the Spin-Liquid Ground State of the $S = 1/2$ Heisenberg Model on the Kagome Lattice," Phys. Rev. Lett. **109**, 067201 (2012).

[25] Andreas M. Läuchli, Julien Sudan, and Roderich Moessner, "$S = \frac{1}{2}$ kagome Heisenberg antiferromagnet revisited," Phys. Rev. B **100**, 155142 (2019).

[26] Alexander Wietek and Andreas M. Läuchli, "Sublattice coding algorithm and distributed memory parallelization for large-scale exact diagonalizations of quantum many-body systems," Phys. Rev. E **98**, 033309 (2018).

[27] M. E. Zhitomirsky, "Field-Induced Transitions in a Kagomé Antiferromagnet," Phys. Rev. Lett. **88**, 057204 (2002).

[28] Tôru Sakai and Hiroki Nakano, "Gapless spin excitations in the S=1/2 Kagome- and triangular-lattice Heisenberg antiferromagnets," Physica B: Condensed Matter **536**, 85 – 88 (2018).

[29] Chisa Hotta and Kenichi Asano, "Magnetic susceptibility of quantum spin systems calculated by sine square deformation: One-dimensional, square lattice, and kagome lattice Heisenberg antiferromagnets," Phys. Rev. B **98**, 140405(R) (2018).

[30] Sho Sugiura and Akira Shimizu, "Canonical Thermal Pure Quantum State," Phys. Rev. Lett. **111**, 010401 (2013).

[31] Jürgen Schnack, Jörg Schulenburg, and Johannes Richter, "Magnetism of the $N = 42$ kagome lattice antiferromagnet," Phys. Rev. B **98**, 094423 (2018).

[32] Marcos Rigol and Rajiv R. P. Singh, "Magnetic Susceptibility of the Kagome Antiferromagnet $ZnCu_3(OH)_6Cl_2$," Phys. Rev. Lett. **98**, 207204 (2007).

[33] Marcos Rigol and Rajiv R. P. Singh, "Kagome lattice antiferromagnets and Dzyaloshinsky-Moriya interactions," Phys. Rev. B **76**, 184403 (2007).

[34] E. F. Shender, V. B. Cherepanov, P. C. W. Holdsworth, and A. J. Berlinsky, "Kagomé antiferromagnet with defects: Satisfaction, frustration, and spin folding in a random spin system," Phys. Rev. Lett. **70**, 3812–3815 (1993).

[35] R. R. P. Singh, "Valence Bond Glass Phase in Dilute Kagome Antiferromagnets," Phys. Rev. Lett. **104**, 177203 (2010).

[36] Ioannis Rousochatzakis, Salvatore R. Manmana, Andreas M. Läuchli, Bruce Normand, and Frédéric Mila, "Dzyaloshinskii-Moriya anisotropy and nonmagnetic impurities in the $s = \frac{1}{2}$ kagome system $ZnCu_3(OH)_6Cl_2$," Phys. Rev. B **79**, 214415 (2009).

[37] S. Dommange, M. Mambrini, B. Normand, and F. Mila, "Static impurities in the $S = 1/2$ kagome lattice: Dimer freezing and mutual repulsion," Phys. Rev. B **68**, 224416 (2003).

[38] Oliver Götze and Johannes Richter, "The route to magnetic order in the spin-1/2 kagome Heisenberg antiferromagnet: The role of interlayer coupling," EPL **114**, 67004 (2016).

[39] I. E. Dzyaloshinskii, "A thermodynamic theory of weak ferromagnetism of antiferromagnetics," J. Phys. Chem. Solids **4**, 241–255 (1958).

[40] T. Moriya, "Anisotropic Superexchange Interaction and Weak Ferromagnetism," Phys. Rev. **120**, 91–98 (1960).

[41] A. Zorko, S. Nellutla, J. van Tol, L. C. Brunel, F. Bert, F. Duc, J.-C. Trombe, M. A. de Vries, A. Harrison, and P. Mendels, "Dzyaloshinsky-Moriya Anisotropy in the Spin-1/2 Kagome Compound $ZnCu_3(OH)_6Cl_2$," Phys. Rev. Lett. **101**, 026405 (2008).

[42] O. Cépas, C. M. Fong, P. W. Leung, and C. Lhuillier, "Quantum phase transition induced by Dzyaloshinskii-Moriya interactions in the kagome antiferromagnet," Phys. Rev. B **78**, 140405(R) (2008).

[43] L. Messio, O. Cépas, and C. Lhuillier, "Schwinger-

boson approach to the kagome antiferromagnet with Dzyaloshinskii-Moriya interactions: Phase diagram and dynamical structure factors," Phys. Rev. B **81**, 064428 (2010).

[44] Laura Messio, Samuel Bieri, Claire Lhuillier, and Bernard Bernu, "Chiral Spin Liquid on a Kagome Antiferromagnet Induced by the Dzyaloshinskii-Moriya Interaction," Phys. Rev. Lett. **118**, 267201 (2017).

[45] Chih-Yuan Lee, B. Normand, and Ying-Jer Kao, "Gapless spin liquid in the kagome Heisenberg antiferromagnet with Dzyaloshinskii-Moriya interactions," Phys. Rev. B **98**, 224414 (2018).

[46] Yin-Chen He and Yan Chen, "Distinct Spin Liquids and Their Transitions in Spin-1/2 XXZ Kagome Antiferromagnets," Phys. Rev. Lett. **114**, 037201 (2015).

[47] Hitesh J. Changlani, Sumiran Pujari, Chia-Min Chung, and Bryan K. Clark, "Resonating quantum three-coloring wave functions for the kagome quantum antiferromagnet," Phys. Rev. B **99**, 104433 (2019).

[48] L. Messio, C. Lhuillier, and G. Misguich, "Lattice sym-

metries and regular magnetic orders in classical frustrated antiferromagnets," Phys. Rev. B **83**, 184401 (2011).

[49] Samuel Bieri, Claire Lhuillier, and Laura Messio, "Projective symmetry group classification of chiral spin liquids," Phys. Rev. B **93**, 094437 (2016).

[50] F. Kolley, S. Depenbrock, I. P. McCulloch, U. Schollwöck, and V. Alba, "Phase diagram of the J_1-J_2 Heisenberg model on the kagome lattice," Phys. Rev. B **91**, 104418 (2015).

[51] Shou-Shu Gong, Wei Zhu, Leon Balents, and D. N. Sheng, "Global phase diagram of competing ordered and quantum spin-liquid phases on the kagome lattice," Phys. Rev. B **91**, 075112 (2015).

[52] Yasir Iqbal, Didier Poilblanc, and Federico Becca, "Spin-$\frac{1}{2}$ Heisenberg J_1-J_2 antiferromagnet on the kagome lattice," Phys. Rev. B **91**, 020402(R) (2015).

[53] Satoshi Nishimoto, Naokazu Shibata, and Chisa Hotta, "Controlling frustrated liquids and solids with an applied field in a kagome Heisenberg antiferromagnet," Nature Communications **4**, 2287– (2013).